Ozone Loss Inside the Northern Polar Vortex During the 1991–1992 Winter

M. H. Proffitt,* K. Aikin, J. J. Margitan, M. Loewenstein, J. R. Podolske, A. Weaver, K. R. Chan, H. Fast, J. W. Elkins

Measurements made in the outer ring of the northern polar vortex from October 1991 through March 1992 reveal an altitude-dependent change in ozone, with a decrease at the bottom of the vortex and a substantial increase at the highest altitudes accessible to measurement. The increase is the result of ozone-rich air entering the vortex, and the decrease reflects ozone loss accumulated after the descent of the air through high concentrations of reactive chlorine. The depleted air that is released out of the bottom of the vortex is sufficient to significantly reduce column ozone at mid-latitudes.

During the Antarctic late winter and early spring, the decrease in ozone (O_3) that is a result of anthropogenic chemical loss is sufficient to overwhelm the naturally occurring increase due to transport of O_3-rich air from lower latitudes (*1*). This dearth of O_3 is obvious in column measurements and has been called an O_3 hole. The seasonal onset of the chemical O_3 loss is not as easily observed because it is masked by increases that are the result of air transport (*2, 3*). In the Northern Hemisphere vortex, the period of significant loss is relatively short because of the warmer, less stable Arctic vortex dissipating by late winter. In this case, a weaker loss is overwhelmed by a stronger seasonal increase that is due to transport (*4, 5*). Although an O_3 hole does not form, the Arctic vortex contains less O_3 than normal.

Concern over O_3 loss recently intensified with reports of significant column O_3 decrease over the heavily populated mid-latitudes in all seasons and both hemispheres (*6*). These mid-latitude changes are not completely understood (*7*), but it appears that the decreases are due to chemistry occurring at mid-latitudes (*8*) and transport of O_3-poor air from polar areas to mid-latitudes (*2, 4, 9, 10*).

In 1991–1992, the second National Aeronautics and Space Administration–National Oceanic and Atmospheric Administration (NASA-NOAA) Airborne Arctic Stratospheric Expedition (AASE II) was undertaken to investigate the cause of the mid-latitude O_3 decreases and to assess the possibility of an ozone hole occurring in the Northern Hemisphere during this century. Daytime measurements of atmospheric chemical and dynamical components were made simultaneously at high latitudes from October 1991 through March 1992. Three flights out of Fairbanks, Alaska (65°N), from 6 to 12 October flew to or near the pole, followed by 17 flights out of Bangor, Maine (45°N), from 12 December through 20 March, eight of which penetrated the polar vortex.

Here, we use AASE II measurements from instruments (*11*) aboard the NASA ER-2 high-altitude aircraft to evaluate offsetting effects of chemical O_3 destruction and transport by analyzing the evolution of chemical species in the outer ring of the winter vortex (*12*). We focus on the vertical distribution of the change in the amount of O_3, the causes of the observed change, and whether loss of O_3 in the polar vortex can account for the winter mid-latitude O_3 decrease.

Ozone is naturally produced and destroyed through photochemistry that occurs in the stratosphere. Before about 1980, the minimum of sunlight that occurs during the polar winter was insufficient to trigger substantial O_3 production or destruction (*13*), but with our present elevated concentrations of stratospheric chlorine, rapid O_3 loss can occur. To distinguish the change in the amount of O_3 (mixing ratio by volume) that results from transport from O_3 loss that is due to chemistry, we adopted a method that uses an empirically derived functional relation between a conserved tracer, nitrous oxide (N_2O) (*14*), and O_3 (*4, 15, 16*). The function is used as a reference for O_3 and represents simultaneous measurements of O_3 and N_2O mixing ratios before wintertime loss has occurred. Because N_2O has a lifetime of years, changes from the reference reflect recent changes in O_3. The difference between a measured value of O_3 and a reference value calculated from the simultaneously measured N_2O represents the wintertime loss (*17*).

Daily meteorological and chemical data show that the vortex perimeter wobbled considerably during AASE II, so identifying its location along each flight leg is critical to our analysis of the vortex interior. The boundary of the polar vortex has been previously defined in a variety of ways, including as (i) a region with large amounts of chlorine monoxide (ClO) (*18*), (ii) the peak in the wind speed (*4*), (iii) threshold values in potential vorticity (*10, 19*) or its maximum gradient (*20*), and (iv) gradients in N_2O and water vapor (*21*). Elevated mixing ratios of reactive chlorine were usually found in the polar vortex (*22*) and indicated significant O_3 destruction was under way. Mixing ratios of the reactive chlorine species ClO were very high on every flight that penetrated the polar jet from December through March (*23*), so we defined the vortex boundary to exclude all data with a mixing ratio of ClO < 150 pptv (parts per trillion by volume) from the vortex interior and to exclude data clearly outside the dynamical boundary (Table 1). Our boundaries are conservative in the sense that some parcels that experience O_3 loss (high ClO) lie slightly outside the boundary, and no air from outside the dynamical vortex is included within the boundary.

For a vertical coordinate, we used potential temperature (a measure of entropy

Table 1. Vortex boundaries and Θ values at the boundaries (*40*). Boundaries were such that the ClO mixing ratio was >150 pptv at all latitudes poleward of the boundary locations (except during dives), and the boundaries were coincident or poleward of steep meridional gradients in N_2O and potential vorticity. N, northbound; S, southbound.

Date	Leg	Boundary latitude (°N)	Boundary Θ (K)	Maximum latitude (°N)
6 Oct.		Prevortex		85
8 Oct.		Prevortex		90
12 Oct.		Prevortex		90
12 Dec.	N	64	480	68
	S	64	490	
4 Jan.	N	59	460	65
	S	57	475	
16 Jan.	N	62	470	69
	S	62	480	
20 Jan.	N	51	460	68
	S	48	495	
13 Feb.	N	57	480	69
	S	55	505	
17 Feb.	N	55	470	69
	S	54	505	
20 Mar.	N	62	500	67
	S	56	520	

M. H. Proffitt and K. Aikin, National Oceanic and Atmospheric Administration Aeronomy Lab, 325 Broadway, Boulder, CO 80303 and Cooperative Institute for Research in Environmental Sciences, University of Colorado, Boulder, CO 80309.
J. J. Margitan, Jet Propulsion Laboratory, California Institute of Technology, Pasadena, CA 91109.
M. Loewenstein, J. R. Podolske, A. Weaver, K. R. Chan, National Aeronautics and Space Administration, Ames Research Center, Moffett Field, CA 94035.
H. Fast, Atmospheric Environmental Service, Downsview, Ontario M3H 5T4, Canada.
J. W. Elkins, National Oceanic and Atmospheric Administration Climate Monitoring and Diagnostics Laboratory, 325 Broadway, Boulder, CO 80303.
*To whom correspondence should be addressed.

and denoted by Θ), which increases with altitude and is calculated from measured temperature and pressure (*24*). In the absence of wave-induced mixing and diabatic cooling, air parcels will stay on surfaces with a constant Θ value (isentropic surfaces). Although altitude is more intuitive as a vertical coordinate, it is less useful at high latitudes during the winter months, particularly when an understanding of transport is required. In our coordinate system, diabatic cooling is equivalent to descent. We defined the bottom of the vortex as $\Theta = 410 \pm 10$ K (*4*), which suggests a relatively free exchange of air with lower latitudes at and below that level (*25*).

The mixing ratio of O_3 increased inside the vortex from October through March by about 1000 ppbv (parts per billion by volume) at all values of Θ (Fig. 1A). However, the steady (isentropic temporal) increase was interrupted by a small decrease in O_3 of about 250 ppbv from December into January below 460 K. From late January through March, the O_3 mixing ratios were nearly constant below 460 K but continued to increase above that level. These increases are due to the transport of O_3-rich air to high latitudes. The result is a 50% increase in the column O_3 between 15 and 20 km from October through mid-February. Over the same period and above 460 K, O_3 mixing ratios also increased substantially relative to mixing ratios of N_2O, but O_3 mixing ratios significantly decreased below that level (Fig. 1B). These changes in the amount of O_3 with a constant N_2O mixing ratios are evident when the raw data of October are compared with the February data (Fig. 2A). The greatest O_3 decrease was found below the bottom of the vortex during the months of January and February (Fig. 2B).

A quadratic fit (*26*) to the October O_3-N_2O data is given by

$$O_3^{OCT} = 1682 + [18.62 \times (N_2O)] - [0.0798 \times (N_2O)^2] \quad (1)$$

with $N_2O > 130$ ppbv and $\sigma = 172$ ppbv (both N_2O and O_3^{OCT} are measured in parts per billion by volume). We use this function as the October reference (*27*). We denote measured mixing ratios of O_3 mixing ratios by O_3^M; thus, the change in O_3 mixing ratios since the October reference period can be simply viewed as the statistical change in the quantity $O_3^M - O_3^{OCT}$. There are three types of air parcels (I, O, and D) that we distinguish by comparison with the October reference:

Type I: $(O_3^M - O_3^{OCT}) > 2\sigma$ (increased O_3)

Type D: $(O_3^M - O_3^{OCT}) < -2\sigma$ (decreased O_3)

Type O: $-2\sigma \leq (O_3^M - O_3^{OCT}) \leq 2\sigma$ (unchanged O_3)

Whether a parcel is type I, O, or D depends on its O_3 content relative to that of N_2O in October (the parcel's initial O_3-N_2O relation) and the photochemical production and loss of O_3 in that parcel since October.

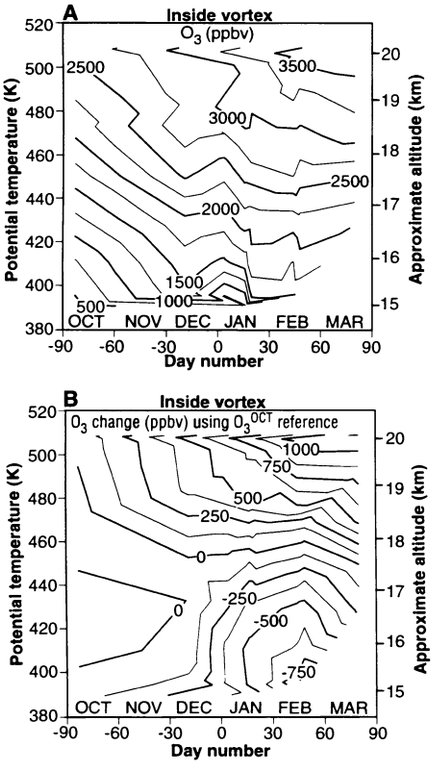

Fig. 1. Evolution of O_3 inside the vortex (*43*). (**A**) Vertical distribution of the O_3 mixing ratio inside the vortex over the period of the mission. (**B**) Change in the O_3 mixing ratio with respect to N_2O (*14*) with the use of the O_3^{OCT} reference. Flights used and vortex boundaries are listed in Table 1. The three October flights are considered as a unit to represent the October O_3 and N_2O data. Data from the other flights in Table 1 were entered into the analyses individually. The approximate altitude was calculated from pressure measurements.

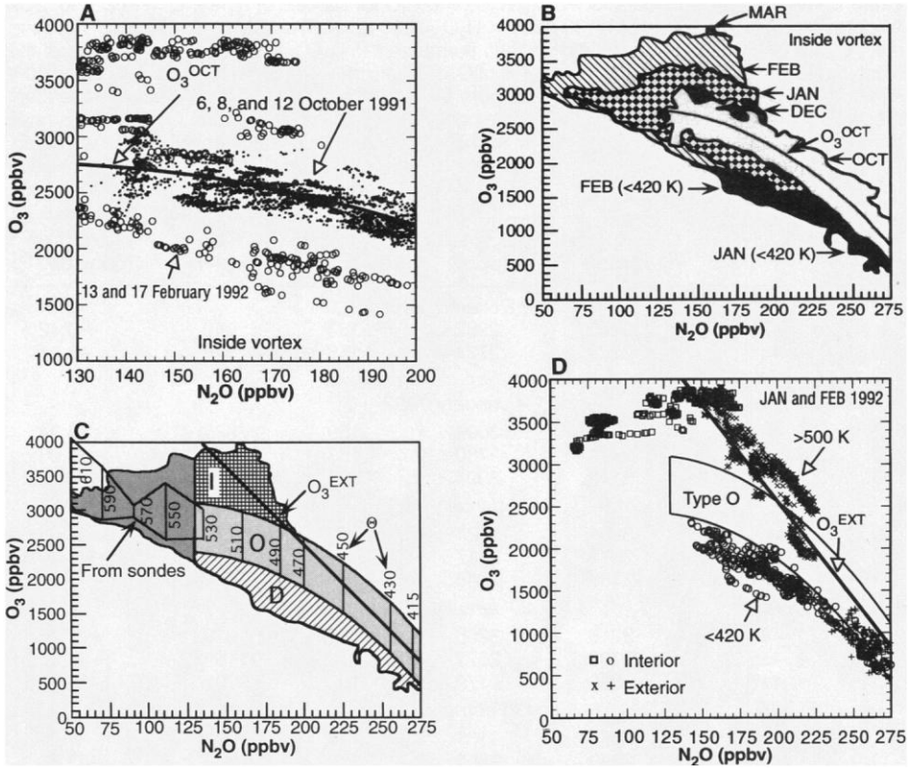

Fig. 2. Plots of O_3 against N_2O during the AASE II mission. (**A**) The three October flights to the pole (small closed circles) are compared with the February data inside the vortex (larger open circles). The heavy line is the O_3^{OCT} reference. (**B**) The outlines of the full range in monthly O_3-N_2O observations inside the vortex are overlaid in a monthly sequence, with data below 420 K indicated for the months of January and February. The O_3^{OCT} reference is also shown. (**C**) The outline of the data in (B) is divided into the parcel types I, O, and D. The average Θ values from 415 to 510 K for the October aircraft data are indicated as vertical bars. The extension of the October O_3-N_2O data to 50 ppbv < N_2O < 130 ppbv is from O_3 sonde and extrapolated aircraft data (*29*). (**D**) Aircraft data from inside and outside the vortex boundary during January and February 1992 are plotted for $\Theta > 500$ K (squares and X's) and $\Theta < 420$ K (circles and pluses).

Parcels of type I have increased amounts of O_3 that must be attributed to photochemical production or to an initial O_3-N_2O relation that differs from the October data—that is, air that was not sampled in October. Ozone production is not responsible for the increase observed because average production rates during the winter are apparently much less than the measured rate of increase (*28*). However, if during October parcels of type I were above altitudes traveled by the ER-2, then descent (decreasing Θ values) in the vortex during the following months might contribute to the increase in O_3. The amount of N_2O generally decreases with increasing values of Θ, and a mixing ratio of $N_2O > 130$ ppbv would not be expected to persist above ER-2 altitudes. As the amount of N_2O decreases, the amount of O_3 is expected to increase at these values of Θ. Simultaneous measurements of N_2O and O_3 mixing ratios at higher values of Θ have never been made at high latitudes in October, so no direct verification is available. In lieu of these measurements, we used O_3 sonde data for October 1991 at five Θ levels from 530 to 610 K for each of two high-latitude stations, Resolute (75°N) and Alert (82°N), which thus verified the increase of O_3 with increasing Θ value. This sonde data along with the ER-2 data allowed us to extend the O_3^{OCT} reference to N_2O mixing ratios of 50 ppbv and Θ = 610 K (*29*) (Fig. 2C). This extended reference implies that neither descent in the vortex nor mixing of higher altitude air ($N_2O < 130$ ppbv) with air of type O can produce the increased O_3 in parcels of type I found in later months. An influx of air from outside the vortex is apparently the only source available for the increase.

To verify this, we compared the O_3-N_2O relation for parcels of type I with a linear fit to the data from December through March from outside the vortex (*30*). The fit is given by

$$O_3^{EXT} = 7172 - [23.06 \times (N_2O)] \quad (2)$$

with $N_2O > 150$ ppbv and σ = 240 ppbv (O_3^{EXT} and N_2O are measured in parts per billion by volume) and agrees well with the O_3-N_2O relation for parcels of type I (Fig. 2C). This suggests that the increase in O_3 mixing ratio is due to air that penetrated the vortex.

A confirmation of this result is provided by the January and February 1992 O_3-N_2O data. If the interior of the vortex were isolated from its exterior at some Θ level, two disjoint O_3-N_2O relations would develop as O_3 increased outside the vortex because of transport and inside was preferentially chemically destroyed. However, we found that for Θ levels accessible to the ER-2, the O_3-N_2O relations were practically indistinguishable over their common range of N_2O mixing ratios (Fig. 2D). At the bottom of the vortex, with $\Theta < 420$ K, air parcels were of type D both inside and outside the boundary and appear as a single line. This is consistent with a relatively free exchange of O_3-poor air latitudinally at and below the bottom of the vortex. At the highest flight level, with $\Theta > 500$ K, the parcels were practically all of type I. Although the two data sets still have identical overlap, they appear as two sharply intersecting lines. This is not consistent with free exchange across the boundary but does indicate that lower latitude parcels penetrated the vortex. Apparently, parcels with an N_2O mixing ratio of about 150 ppbv had recently entered at this level and still had their exterior character, whereas other parcels had apparently mixed with vortex air of lower N_2O content. This produced the line of vortex data characteristic of mixing (Fig. 2D). Although not shown in our figures, all isentropic levels above the bottom of the vortex were similar to the level with values of $\Theta > 500$ K and show distinct, somewhat linear data sets with common overlap. This indicates that air penetrated the vortex at all flight altitudes.

We found virtually no air parcels with a mixing ratio of $N_2O < 140$ ppbv outside the vortex boundary (*31*), which indicates that air deep inside the vortex with a mixing ratio of $N_2O << 140$ ppbv did not escape the vortex and retain its identity in the process. This does not exclude vortex peel-off (*10*) as a contributor to vortex edge material at mid-latitudes. Parcels of type D contain less O_3, which must be attributed to photochemical loss or to an initial O_3-N_2O relation below the O_3^{OCT} reference. Diabatic cooling (descent) rather than diabatic heating dominated throughout the period, and descent inside the vortex without O_3 loss increased rather than decreased amounts of O_3 relative to N_2O (Fig. 1B). Air outside the vortex is rich in O_3 and cannot directly account for the decrease. We conclude that the dom-

Table 2. Averages of 10-s data for Θ, O_3, N_2O, and ClO for parcels of type I, O, and D (Fig. 2C). All data are inside the vortex with 130 ppbv < N_2O < 180 ppbv. The calculated value of O_3 mixing ratio, O_3@155, is the average O_3 mixing ratio normalized to N_2O = 155 ppbv with the use of the measured value for $d(O_3)/d(N_2O)$. Loss rates of O_3 [$d(O_3)/(dt)$] were calculated from averaged 10-s measurements of $[ClO]^2$; we assumed 6 hours of daily solar exposure and altitude-dependent bromine monoxide (BrO) mixing ratios that are consistent with 1989 AASE data (*41*). The loss rates represent the forward rate of ClO dimer formation along with the reactions of ClO with BrO. Temperature-dependent rate constants are from the 1992 Jet Propulsion Laboratory compilation (*42*).

Parcel type	Θ (K)	O_3 (ppbv)	O_3@155 (ppbv)	N_2O (ppbv)	ClO (pptv)	$d(O_3)/dt$ (ppbv day^{-1})
			12 December 1991			
I	477	3035	2982	153	340	−3.42
O	464	2774	2774	155	348	−3.84
D	No data					
			4 January 1992			
I	472	3001	3094	159	886	−14.34
O	464	2724	2780	163	698	−11.06
D	424	2114	2394	177	475	−8.06
			16 January 1992			
I	478	3201	2921	142	737	−11.03
O	464	2875	2817	144	768	−13.14
D	431	2189	2245	159	654	−12.82
			20 January 1992			
I	493	3218	3256	157	929	−13.72
O	455	2733	2677	144	1105	−25.45
D	417	2096	2179	162	702	−17.80
			13 February 1992			
I	487	3372	3181	146	383	−4.76
O	462	2930	2852	139	796	−13.86
D	427	2054	2104	159	693	−15.25
			17 February 1992			
I	507	3750	3773	156	180	−1.48
O	468	2833	2815	152	308	−3.42
D	416	1969	1996	157	509	−9.82
			20 March 1992			
I	505	3654	3856	164	163	−1.40
O	451	2629	2627	154	146	−1.41
D	No data					

inant cause of the decrease in O_3 must be photochemical O_3 loss that has occurred during winter.

Why was the amount of O_3 constant at 460 K? Diabatic cooling was taking place, so air with enhanced O_3 must have descended through the 460 K isentrope. This should have increased O_3 relative to N_2O, so lack of change represents a close balance between the increase due to transport (including descent) and photochemical loss. Transport similarly masks O_3 loss at all levels throughout the outer vortex.

To quantify the offsetting effects of transport and photochemical O_3 loss, we calculated average daily loss rates, flight-by-flight, from December through March for air parcels of types I, O, and D (Table 2). We assumed conservatively only 6 hours of daily solar exposure and restricted N_2O to mixing ratios common to all three parcel types (Fig. 2C). A relatively weak O_3 loss began by mid-December (Fig. 3A). In early January, the rate of O_3 destruction increased substantially and was greatest in parcels of type I. By mid-January, the destruction rate was greatest for parcels of type O and D, although the mixing ratios of ClO were comparable (*32*) (Table 2). By mid-February, the O_3 destruction in type I parcels had decreased significantly but remained relatively high for types O and D. This is because (i) air parcels initially of type I lost O_3 and became parcel types O and D and (ii) relatively unprocessed air of type I (that is, containing smaller amounts of reactive chlorine) had been transported into the vortex and hence had a lower O_3 destruction rate. Comparison of the calculated O_3 loss rates with the measured rates of O_3 change (Table 2) show that the measured rates underestimate loss in all parcel types (Fig. 3, A and B). Transport-induced increases even dominated the significant loss rates calculated at the highest levels.

Although much is understood about high-latitude O_3 photochemistry, our understanding of polar vortex dynamics is far from complete and the topic is somewhat controversial. The dispute began for the Antarctic and extended to the Arctic, concentrating on whether the vortex is an isolated air mass (*33*) or not (*2, 4, 21, 34*). Advocates of the isolation theory argue that both polar vortices define a region of highly isolated air (*35*) and that polar loss has virtually no effect on mid-latitude O_3 mixing ratios before the vortex breaks up. They also argue there is one-way transport from the vortex edge to mid-latitudes as the vortex erodes. The opposing view contends that the vortex is a flowing processor, with O_3-rich air entering and depleted or processed air (that is, air with larger amounts of reactive chlorine) leaving the vortex region. Supporters of the flowing processor claim that replenishment of vortex O_3, descending flow through the vortex, and the peeling off of processed edge material must be accounted for to accurately evaluate the mass of O_3 destroyed because of polar processes and the subsequent dilution of O_3 at lower latitudes (*2*). The flowing processor has been criticized with dynamical arguments that claim that poleward fluxes into the vortex are not significant (*35, 36*).

The change in O_3 mixing ratio over the winter months can be conservatively estimated directly from the O_3^{OCT} reference inside and outside the vortex at various Θ levels (Fig. 4A). The O_3^{OCT} reference ignores poleward transport as required for an isolated vortex. If, instead, we assume there was sufficient poleward flow of air into the outer ring of the vortex to replace the October air with exterior air, then O_3 loss accumulated over the period would be better estimated with O_3^{EXT} as the reference (Fig. 4B). This approach is considered as an upper limit for the loss accumulated, particularly for December when parcels remaining from October might still be descending through the vortex. The O_3^{OCT} analysis indicates that only small isentropic gradients in O_3 change when crossing into the vortex, whereas the O_3^{EXT} analysis reveals the abrupt increase in loss expected in the region of highly elevated reactive chlorine. Although no loss was found above 460 K with the use of the O_3^{OCT} reference, the loss calculated

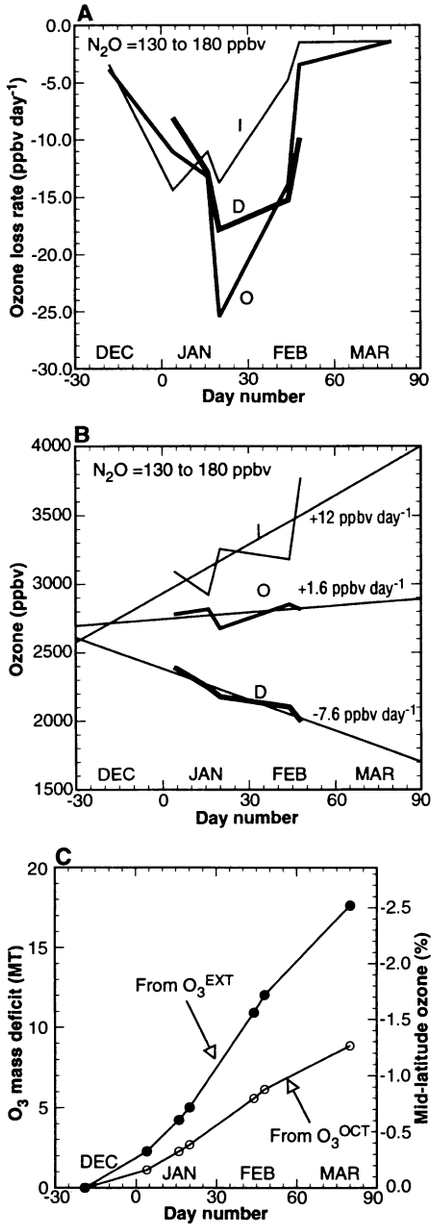

Fig. 3. (**A**) Calculated daily O_3 loss rates (Table 2). (**B**) Values for the calculated O_3 mixing ratio, O_3@155 (Table 2), from 4 January through 17 February, with linear fits to the data from parcel types I, O, and D. The slopes of the lines represent measured daily O_3 loss rates. (**C**) O_3 mass deficit in the air released from the bottom of the vortex.

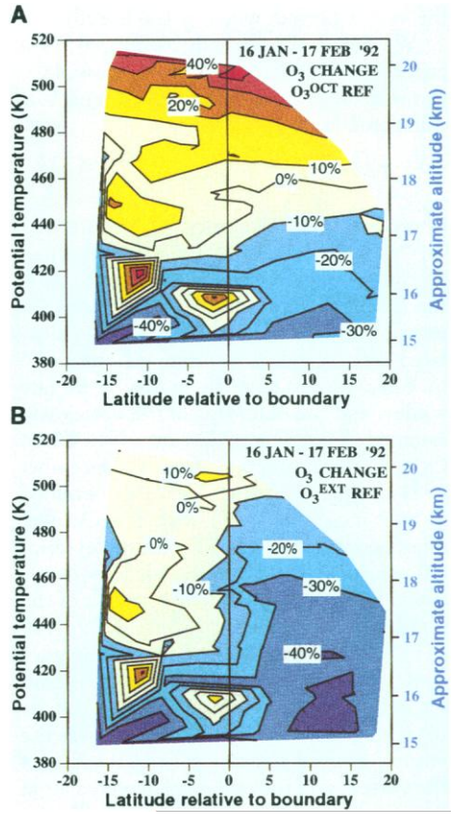

Fig. 4. Cross section through the vortex boundary of the percent change in O_3 referenced through (**A**) O_3^{OCT} and (**B**) O_3^{EXT}. Data with N_2O > 130 ppbv from the four flights of 16 January through 17 February were taken as a unit then averaged to produce the contour (*43*). The horizontal coordinate was averaged over 1° of latitude.

with O_3^{EXT} (Fig. 4B) compares well with the 25% loss at 18 km obtained from AASE II lidar measurements (*25*) and with the 20% loss at Θ = 470 K, calculated with a photochemical model that used AASE II measurements and meteorological tracer data (*37*). However, the larger decrease we found at lower Θ levels (using both references) and the mixture of depleted and enhanced O_3 we found at and below the bottom of the vortex outside its boundary (Fig. 4B) have not been reported by others. The altitude distribution of O_3 decrease outside the vortex is consistent with the altitude distribution of the long-term decrease reported from sonde and from satellite measurements (*38*). Figure 4B portrays a vortex that is not an impenetrable container nor completely unconstrained with no sides and no bottom. For each Θ level outside the boundary, the vortex can be pictured as a leaky bucket: fluid enters the bucket over the lip (air enters the vortex at a Θ level) and the walls of the bucket restrict the fluid as it descends and mixes with fluid already in the bucket (air descends and mixes inside the vortex) until it exits through the leaky bottom (until it reaches the vortex bottom where it is released).

We define the O_3 mass deficit, ϑ, of a portion of the atmosphere as the mass of O_3 lost relative to a reference O_3 content; it is calculated as

$$\vartheta = k\int[w \times A \times (O_3^{M} - O_3^{REF}) \times \rho]dt \quad (3)$$

where ρ is the air density, O_3^{REF} is either O_3^{OCT} or O_3^{EXT}, w is the rate of parcel descent at the bottom of the vortex, A is the area of descent, and k is a constant (in units of mass per O_3 molecule). We calculated vertical velocities from -70 m day^{-1} in early winter to -55 m day^{-1} in late winter, and the outer ring of the vortex was assumed as the area of descent (*39*). When O_3 loss is thus integrated from 12 December 1991 through 20 March 1992, we obtained ϑ = 9 megatons (MT) with the October reference and ϑ = 18 MT with the exterior reference (Fig. 3C). These deficits correspond to 1.3 and 2.6%, respectively, of the total mass of O_3 from 30° to 60°N (700 MT), a significant part of the 4% average wintertime mid-latitude decrease in column O_3 amount observed over the past decade (*6*). Descending air that is deeper inside the vortex, air that is spun off from the side of the vortex, and the release of depleted air at the time of the vortex demise will also contribute to the O_3 mass lost at high latitudes.

REFERENCES AND NOTES

1. J. G. Anderson *et al.*, *J. Geophys. Res.* **94**, 11480 (1989); J. Austin *et al.*, *ibid.*, p. 16717; J. G. Anderson, W. H. Brune, M. H. Proffitt, *ibid.*, p. 11465.
2. M. H. Proffitt *et al.*, *ibid.*, p. 16797.
3. J. W. Waters *et al.*, *Nature* **362**, 597 (1993).
4. M. H. Proffitt *et al.*, *ibid.* **347**, 31 (1990).
5. R. D. Bojkov, *Meteorol. Atmos. Phys.* **38**, 117 (1988).
6. R. Stolarski *et al.*, *Science* **256**, 342 (1992).
7. "WMO/UNEP Global Ozone Research and Monitoring Project Report No. 25, Executive Summary" (World Meteorological Organization, Geneva, 1991).
8. J. M. Rodriguez, M. K. W. Ko, N. D. Sze, *Nature* **352**, 134 (1991); D. W. Fahey *et al.*, *ibid.* **363**, 509 (1993); D. J. Hofmann and S. Solomon, *J. Geophys. Res.* **94**, 5029 (1989).
9. R. J. Atkinson, W. A. Matthews, P. A. Newman, R. A. Plumb, *Nature* **340**, 290 (1989); S. J. Reid and G. Vaughan, *Q. J. R. Meteorol. Soc.* **117**, 825 (1991).
10. A. F. Tuck *et al.*, *J. Geophys. Res.* **97**, 7883 (1992).
11. Instruments are described in the following: M. H. Proffitt *et al.*, *ibid.* **94**, 16547 (1989); W. H. Brune, J. G. Anderson, K. R. Chan, *ibid.*, p. 16649; K. R. Chan *et al.*, *ibid.*, p. 11573; M. Loewenstein, *ibid.*, p. 11589; and J. W. Elkins *et al.*, *Eos* **73**, 106 (1992).
12. The vortex interior has two different aspects: (i) an outer ring generally within or near the polar night jet and characterized by high wind speeds and intermittent sunlight and (ii) an inner vortex usually at the highest latitudes (nearer the pole) with much lower wind speeds and much less sunlight. Most of the flights during AASE II did not penetrate the inner vortex; therefore, the data are considered as representative of the outer vortex.
13. L. M. Perliski, S. Solomon, J. London, *Planet. Space Sci.* **37**, 1527 (1989).
14. Data for N_2O were not available for 20 March, so another conserved tracer, chlorofluorocarbon trichlorofluoromethane (CFC-11), was used in its place.
15. M. H. Proffitt, D. W. Fahey, K. K. Kelly, A. F. Tuck, *Nature* **342**, 233 (1989).
16. M. H. Proffitt, S. Solomon, M. Loewenstein, *J. Geophys. Res.* **97**, 939 (1992).
17. Loss of O_3 occurs naturally during the summer at high latitudes [J. C. Farman *et al.*, *Q. J. R. Meteorol. Soc.* **111**, 1013 (1985)] and must be considered when wintertime loss is evaluated. If this O_3-poor air becomes trapped at high latitudes during vortex formation in early November and remains as an isolated pool through January and February, the reference function must represent the fall O_3-N_2O relation.
18. M. H. Proffitt *et al.*, *J. Geophys. Res.* **94**, 11437 (1989).
19. M. R. Schoeberl *et al.*, *Geophys. Res. Lett.* **17**, 469 (1990).
20. L. R. Lait *et al.*, *ibid.*, p. 521.
21. A. F. Tuck, *J. Geophys. Res.* **94**, 11687 (1989).
22. C. R. Webster *et al.*, *Science* **261**, 1130 (1993).
23. D. W. Toohey *et al.*, *ibid.*, p. 1134.
24. Values for Θ are calculated by $T(1000/P)^{0.286}$, where T is temperature in kelvin and P is pressure in millibars.
25. E. V. Browell *et al.*, *Science* **261**, 1155 (1993).
26. The fit was obtained from 10-s data taken on 6, 8, and 12 October 1991. The O_3 and N_2O measurements were averaged into eight equal Θ ranges from 360 to 520 K, and a quadratic fit to these averages was calculated, thus weighting the data equally by Θ value. An unweighted fit was compared and found to be almost identical except at the highest N_2O mixing ratios, where the O_3 mixing ratio was about 10% higher in the unweighted fit.
27. Air with N_2O < 130 ppbv was not accessible to the ER-2 early in the mission, but diabatic cooling brought much lower values within aircraft altitudes during January and February. Accordingly, parcels with N_2O < 130 ppbv are excluded from all comparisons with the October reference.
28. D. S. McKenna *et al.*, *Geophys. Res. Lett.* **17**, 553 (1990).
29. Monthly averages of O_3 sonde data for October 1991 are calculated at five Θ levels from 530 to 610 K for each of the two high-latitude stations [Resolute (75°N) and Alert (82°N)], thus providing some station-to-station variability. We estimated the amount of N_2O for the same five Θ levels by extrapolating a quadratic fit to the October N_2O-Θ aircraft data. The Θ value has been limited to 610 K because the extrapolation implies that the average N_2O mixing ratio at 610 K is 50 ppbv; therefore, this value for Θ is an extreme limit for finding air with N_2O > 130 ppbv.
30. This exterior reference is calculated from 10-s data that are more than 2° of latitude outside the boundary of the vortex and with Θ > 420 K. Data within 2° were excluded to avoid contamination of the exterior data with vortex data that fall outside our conservative choice for a vortex boundary; the Θ values chosen were > 420 K to exclude air parcels coming out of the bottom of the vortex. Equation 2 is practically identical to the fit to the 1989 AASE exterior data.
31. On only one occasion (17 February) did we find air parcels with N_2O < 140 ppbv outside the vortex boundary (<1° outside). These parcels had the character of vortex air.
32. This is primarily because the loss rate is nearly proportional to the square of the air density, therefore producing an enhanced loss at the higher pressures in type D and O parcels [D. M. Murphy, *J. Geophys. Res.* **96**, 5045 (1991)].
33. M. N. Jukes and M. E. McIntyre, *Nature* **328**, 590 (1987); D. L. Hartmann *et al.*, *J. Geophys. Res.* **94**, 16779 (1989); M. R. Schoeberl and D. L. Hartmann, *Science* **251**, 46 (1991).
34. E. F. Danielsen and H. Houben in *Anthropogene Beeinflussung der Ozonschicht*, D. Behrens and J. Wiesner, Eds. (Herausgeber, Frankfurt, 1988), for DECHEMA (Deutsche Gesellschaft für Chemisches Apparatewesen, Chemische Technik und Biotechnologie e.V.) p. 191.
35. M. R. Schoeberl *et al.*, *J. Geophys. Res.* **97**, 7859 (1992).
36. A. Plumb, *Nature* (News & Views) **347**, 20 (1990).
37. R. J. Salawitch *et al.*, *Science* **261**, 1146 (1993).
38. M. P. McCormick, R. E. Veiga, W. P. Chu, *Geophys. Res. Lett.* **19**, 269 (1992). They report statistically significant (2σ) decreases below 18 and 19 km, respectively, and show negative trends increasing down to 15 km.
39. The rate of descent at the bottom of the vortex (w) can be estimated by assuming diabatic cooling rates of 1 K day^{-1} multiplied by the measured vertical gradients in Θ. Because most of the data are in the outer ring, the area of descent (A) has been limited to 1.2 × 10^{13} m^2, an area equivalent to that from 65°N to 72°N, or approximately half the area of the vortex. The mixing ratio of N_2O at the bottom of the vortex was >150 ppbv and thus within the range for the functions defining O_3^{OCT} and O_3^{EXT}. Our calculations result in a conservative estimate of total O_3 mass destroyed.
40. A flight on 6 January 1992 also penetrated the polar vortex, but data were not available from all of the instruments.
41. D. W. Toohey *et al.*, *Geophys. Res. Lett.* **17**, 513 (1990).
42. Publication 92-20, Jet Propulsion Laboratory, Pasadena, CA (1990).
43. Contour plots were produced with DeltaGraph Professional (version 2.0.2) software (Deltapoint, Inc., Monterey, CA). The contoured data were averaged into seven equal Θ ranges from 380 to 520 K. All data are plotted without smoothing and usually appear as sharp corners. The data were equally weighted with linear interpolations on triangular grids between data points to span the gaps.

44. We thank J. G. Anderson, D. W. Toohey, L. M. Avallone, L. R. Lait, P. A. Newman, M. R. Schoeberl, E. Danielsen, D. W. Fahey, and A. F. Tuck for their contributions.

19 February 1993; accepted 25 June 1993